Estimating the Albedo of Urban Materials through the Bidirectional Reflectance Distribution Function

Tserepis Marios (ph4926)

University of Crete, Department of Physics

Heraklion, 19/06/2024

Supervisors:

Charmandaris Vassilis

Chrysoulakis Nektarios

Mitraka Zina

Contents:

Introduction: Cities have their own microclimates, which are influenced by a variety of factors. Some of these are the materials used for buildings and roads, the height and density of building, and the shapes of surfaces. This microclimate can have a significant impact on the temperature inside cities compared to rural areas, which can cause heat stress related problems for their residents[1]. The albedo of the materials is of particular importance, because it determines the total amount of radiation that is reflected by them. The remaining light that isn't reflected by the material, is instead absorbed by it, thus increasing their temperature[2]. Therefore, it is important to understand the radiative properties of materials, the way these are connected to the shape of their surface, and their albedo. This can be achieved by measuring the radiance leaving the materials using a hyperspectral radiometer, which is able to capture a wide and continuous range of wavelengths. In this study, a method was developed to derive the albedo of materials by calculating the Bidirectional Reflectance Distribution Function (BRDF) using hyperspectral measurements taken under direct sunlight, and it was used to calculate the albedo for materials used in the city of Heraklion.

Theoretical Background: The way materials reflect light depends on multiple factors, such as the surface of the material, the material itself, and the location of the light source. The incoming solar radiation depends on the weather conditions, as clouds obstruct the paths of photons, humidity and atmospheric aerosols[3], which interact with certain wavelengths. Despite this complexity, it is possible to measure the spectral reflectance of a material, by measuring the material's radiance for each wavelength (figures 1B through 1D), and also measuring the radiance of each wavelength of a 99% reflectance diffuse panel in the same spot under the same conditions (figure 1A), assuming the panel is Lambertian. A Lambertian surface is one which reflects light homogenously and isotopically, so measuring the reflected light from this surface allows me to calculate the incoming solar radiation.
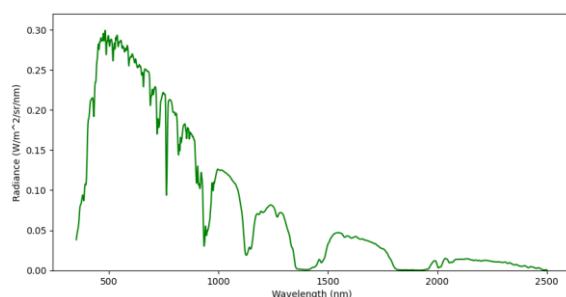
A)
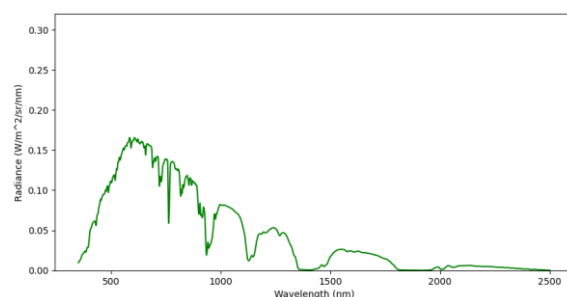
B)
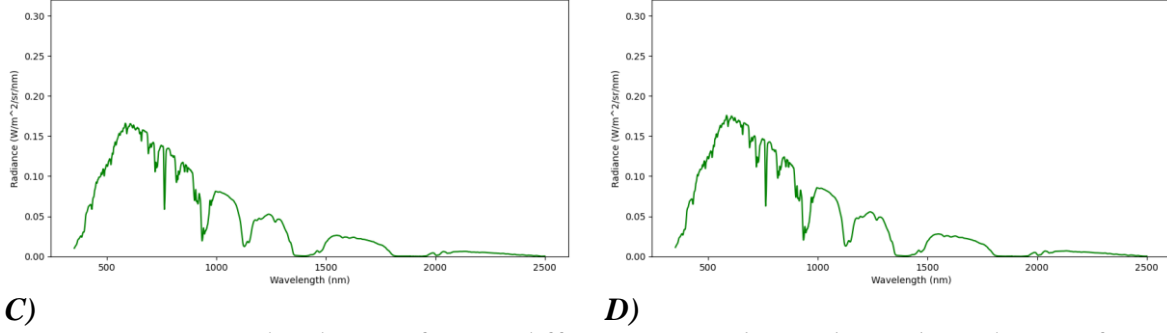
C)   *D)*

Figure 1) Measured radiances for two different materials. A) shows the radiance of a spectral diffuse panel measured at θ=0°, B) C) and D) show a cement plate, with B) being measured at θ=0°, C) being measured at θ=30° and φ=315°, and D) being measured at θ=60° and φ=315°

Figure 1A shows the radiance of a spectral diffuse panel, which was used as a Lambertian surface in our measurements, and figures 1B through 1D show the radiances of a cement plate. All of these measurements were done in the same day, within minutes of each other, so the sun's position in the sky and the atmospheric conditions were practically identical. The radiances measured at a zenith angle of 0° and 30° are slightly different, while the one measured at 60° is noticeably higher. Comparing the radiance of the Lambertian to those of the material, it is immediately apparent that a large portion of incoming radiation is not reflected by the material. It's also important to note that in certain spectral wavelengths, the measured radiance is close to zero.

The spectral reflectance $r(\theta, \varphi, \theta_0, \varphi_0, \lambda)$ of the material for the specific view angle can be calculated with the following sum[4].

$$r(\theta, \varphi, \theta_0, \varphi_0, \lambda) = \frac{S^\uparrow(\theta, \varphi, \theta_0, \varphi_0, \lambda)}{S^\downarrow(\theta_0, \varphi_0, \lambda)} = \frac{S^\uparrow(\theta, \varphi, \theta_0, \varphi_0, \lambda)}{S_L(\theta, \varphi, \theta_0, \varphi_0, \lambda)/SRF_L(\theta, \varphi, \theta_0, \varphi_0, \lambda)} \quad (1)$$

Where $S^\uparrow(\theta, \varphi, \theta_0, \varphi_0, \lambda)$ is the reflected radiance, $S^\downarrow(\theta_0, \varphi_0, \lambda)$ is the incoming radiance, $S_L(\theta, \varphi, \theta_0, \varphi_0, \lambda)$ is the radiance reflected by the spectral diffuse panel, and $SRF_L(\theta, \varphi, \theta_0, \varphi_0, \lambda)$ is the spectral response factor of the spectral diffuse panel.

The measurements were done under direct sunlight, so in order to account for the potentially variable conditions of the atmosphere, such as moving clouds, atmospheric aerosols, or dust, each spot was measured N times, and after calculating the mean value for each wavelength $\overline{S}(\theta, \varphi, \theta_0, \varphi_0, \lambda)$, the following sum was used to calculate the standard deviation $STD(\theta, \varphi, \theta_0, \varphi_0, \lambda)$ of the set of measurements[4]:

$$STD(\theta, \varphi, \theta_0, \varphi_0, \lambda) = \sqrt{\frac{1}{N}\sum_{k=1}^{N}\left(S_k(\theta, \varphi, \theta_0, \varphi_0, \lambda) - \overline{S}(\theta, \varphi, \theta_0, \varphi_0, \lambda)\right)^2} \quad (2)$$

This quantity can be used for certain λ to make a criterion for accepting or rejecting sets of measurements. The criterion is the following[4]:

$$\frac{1}{(\lambda_n-\lambda_1+1)}\sum_{\lambda=\lambda_1}^{\lambda_n}\frac{STD(\theta,\varphi,\theta_0,\varphi_0,\lambda)}{\bar{S}(\theta,\varphi,\theta_0,\varphi_0,\lambda)} \leq 0.03 \quad (3)$$

For every set of measurements that fulfills this criterion, the average spectral reflectance $\bar{r}(\lambda)$ will be calculated and presented in groups of materials. The broadband reflectance is calculated with the following integral:

$$\rho(\theta,\varphi,\theta_0,\varphi_0) = \frac{\int_{\lambda_1}^{\lambda_2}(S^\uparrow(\theta,\varphi,\lambda)d\lambda)}{\int_{\lambda_1}^{\lambda_2}(S^\downarrow(\theta_0,\varphi_0,\lambda)d\lambda)} \quad (4)$$

The broadband reflectance is determined by the Bidirectional Reflectance Distribution Function (BRDF), which is a function of the locations of the measurement and the light source. It defines the following relationship between the incident radiance from a specific direction $S^\downarrow(\theta_0,\varphi_0)$ and reflected radiance in another direction $S^\uparrow(\theta,\varphi)$[5]:

$$S^\uparrow(\theta,\varphi) = \int_{2\pi}\int_{\pi/2}S^\downarrow(\theta_0,\varphi_0)BRDF(\theta,\varphi,\theta_0,\varphi_0)\cos(\theta_0)\sin(\theta_0)\,d\theta_0\,d\varphi_0 (5)$$

Where $BRDF(\theta,\varphi,\theta_0,\varphi_0,)$ is the BRDF, θ is the view zenith angle, φ is the view azimuth angle, θ_0 is the incident light zenith angle, and φ_0 is the incident light azimuth angle. The broadband reflectance can also be called the Bidirectional Reflectance Factor (BRF), which is connected to the BRDF via the following relationship[6]:

$$\rho(\theta,\varphi,\theta_0,\varphi_0) = \pi \cdot BRDF(\theta,\varphi,\theta_0,\varphi_0)(6)$$

In this work the BRDF will be approximated using machine learning methods. Due to strong atmospheric absorption in certain spectral bands (1345 nm–1475 nm, 1780 nm–2025 nm, and 2340 nm–2500 nm)[4], which are also visible in figure 1, these wavelengths are removed from all calculations, as the measurements for them are mostly noise.

The albedo of a material is defined as the ratio of outgoing radiation flux divided by the incoming radiation flux in a hemisphere above the surface of the material[2]. The broadband albedo α, or simply albedo, is the ratio of total radiative fluxes, while the spectral albedo α_λ is the albedo for monocrhomatic radiation at wavelength λ [2]. Both of these values depend on the reflective properties of the material, the shape of the material, the location of the sun, and

the conditions of the atmosphere. In this work, the broadband albedo will be estimated, which can be done using the BRDF by the following integral[7]:

$$\alpha = \pi^{-1} \int_{2\pi} \int_{\pi/2} \rho(\theta,\varphi)\cos\theta\,\sin\theta d\theta d\varphi \quad (7)$$

Where α is the albedo, θ is the view zenith angle, φ is the relative azimuth angle between the measurement and the sun, and ρ(θ,φ) is the BRDF for a single location of the sun. This integral can be approximated by calculating the following sums[6]:

$$\alpha \approx \pi^{-1} \sum_{j=1} \rho_j \,\Delta\Omega_j \quad (8)$$

$$\rho_j = \sum_{k=1}^{m} \rho(\theta_j^*,\varphi_k)/m \,, \theta_{j-1} < \theta_j^* < \theta_j \quad (9)$$

$$\Delta\Omega_j = \pi\big(\sin^2(\theta_j) - \sin^2(\theta_{j-1})\big) \quad (10)$$

Equipment: In order to measure radiation, the RS-3500 hyperspectral radiometer was used. It detects wavelengths from 350 nm to 2500 nm, with a spectral resolution of 1 nm. Its field of view (FOV) is 25°. A white spectral diffuse panel was used as a Lambertian surface. Knowing the spectral response factor of this panel makes it possible to calculate the incoming solar radiation. Every campaign was conducted in sunny weather, with little to no clouds, to minimize the variability of the incoming radiation. The radiometer is also equipped with a GPS and clock, which are used to calculate the position of the sun in the sky for every measurement.

Figure 2) The radiometer and the spectral diffuse panel

Methodology: The first step is to define a reference system for taking measurements. The x axis points towards the north, the y axis points towards the west, and the z axis is perpendicular to the surface, facing upwards. Figure 3 shows the reference system, along with all relevant angles.
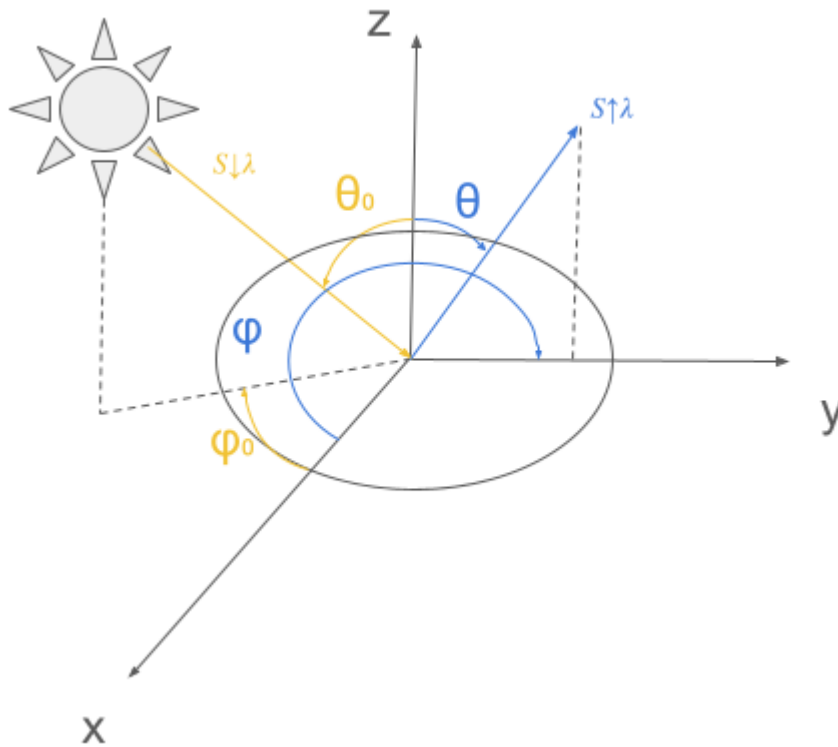

Figure 3

The measurement process is the following. First, the radiometer is placed at $\theta=0°$, which is directly above the surface of the material, and N measurements are taken. Then, the radiometer is set to $\theta=30°$. Starting at $\varphi=0°$, N measurements are taken, and the radiometer's azimuth angle is moved clockwise by 45° in the clockwise direction. After completing one azimuth circle around the material, the radiometer is set to $\theta=60°$, and another azimuth circle is measured. Under certain azimuth angles the radiometer's shadow would be obstructing the measurement. Every angle for which this was the case was skipped. N measurements of the diffuse panel are also taken at $\theta=0°$ once during this process.

Initially, N=5 was chosen, with each measurement lasting 4 seconds. However, this was very time-consuming, so N=3 was considered, with each measurement lasting 3 seconds. To compare the reliability of the two methods, a material was picked, and at a single zenith angle of the radiometer, two azimuth circles were measured, one for each of the two methods. The largest difference between two values is 0.011, which is 3.4% of the smallest measured value. Thus, the two methods of measurement are equally reliable, so the rest of the measurement

process was done with 3-second measurements and 3 averages in order to speed up the process. Using this method, the process of measuring one dome around the material takes around 15 minutes to complete. This process is done at various times of the day and on various days to obtain measurements for different solar angles.
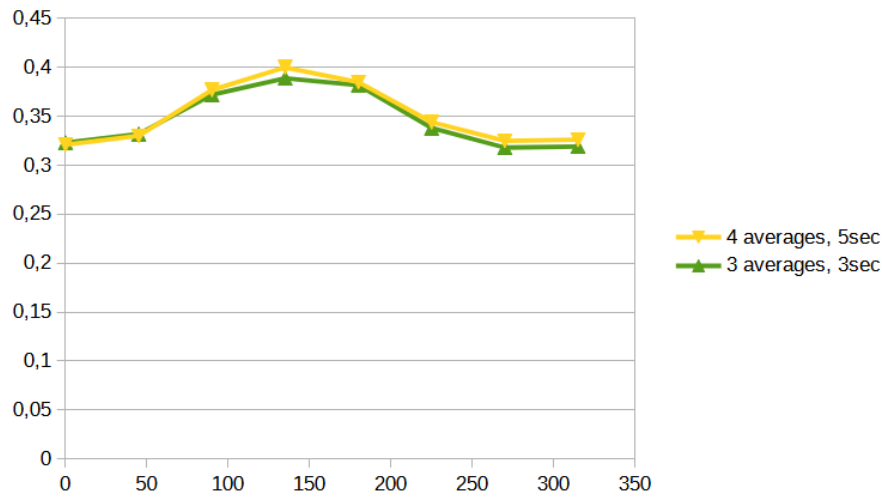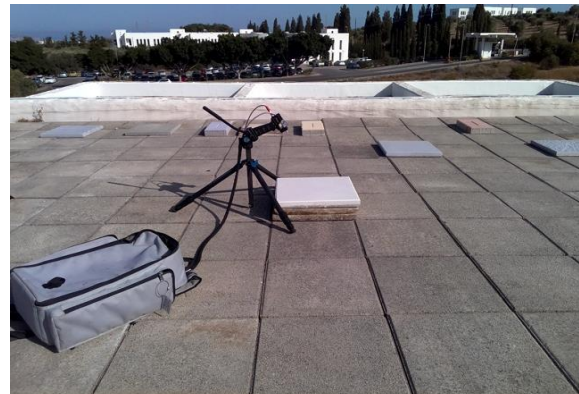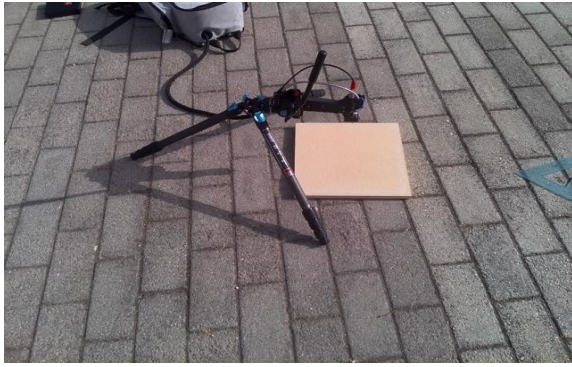

Figure 4)
Comparison of two azimuth seconds recorded in the same day using the two measurement settings


A)

B)

C)

D)

E)

F)

*Figure 5) The materials that were measured*

Figure 5 shows the materials that were measured. Figure 5A shows a grey cement plate, figure 5B shows a white cement plate, figure 5C shows a yellow cement plate, figure 5D shows a ceramic plate that is used in roofs, figure 5E shows some grass, and figure 5F shows some asphalt. The grey and white cement plates were made from the same material but had a different coat of paint. The yellow cement plate was made from a different material than the other two. All of these plates were level, with the grey and white plates having a fine-roughness, and the yellow plate being smoother than the other two. The ceramic surface also had a fine-roughness on its surface but was also heavily curved. In the measurement process, the ceramic surface was oriented along the x axis. The grass' surface is very complex, and the asphalt's surface was weathered, which made it smoother than new asphalt, but still rough.

After the measurements were gathered, the next step was to fit them to an SVR algorithm that would model the BRDF of the materials. An SVR algorithm is a machine learning method used to perform regression of data of arbitrary dimention[8]. It was chosen because of its ease of use, because it only requires up to three variables, and is guaranteed to fit to the data in some form. However, such an algorithm would require many more measurements than the ones collected, so a two-step process was devised. First, each material's measurements

were separated to two datasets, one which had all measurements at a 0° view angle, which didn't require further processing, and another with the rest of the measurements, which was further separated for each azimuth circle measured. More specifically, these measurements are the ones that were done with θ=30° and θ=60°. Since the points were measured along one azimuth circle around the material with these zenith angles, the dataset can be split between each of these azimuth circles, each with both the sun and the instrument's zenith angle in a different location. Each of the azimuth circles was treated individually. Two of these circles were chosen randomly, one at 30° and one at 60°, to set aside and use to validate the final brdf models. However, due to the importance of the maximum reflectance for the models, a circle wouldn't be placed in the validation dataset if it contained the largest measured broadband reflectance. The rest of the data would be fit to a 2D SVR algorithm which would predict the broadband reflectance using the angle, effectively increasing our azimuth angular resolution from 45° to 1°. To achieve this, the broadband reflectance measured at 0° was added to a new point at 360° with the same broadband reflectance. Additionally, every measurement that was skipped due to the shadow of the radiometer was extrapolated to be the average of the two neighboring values. Figure 6 shows some plots of the SVR buffed satasets.
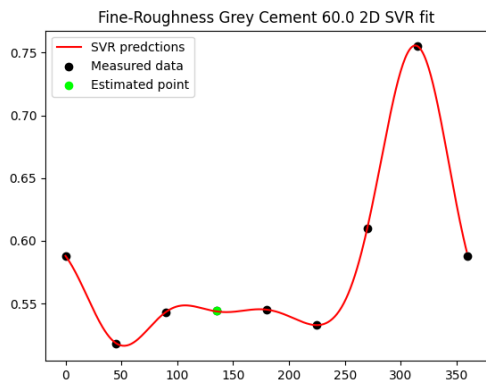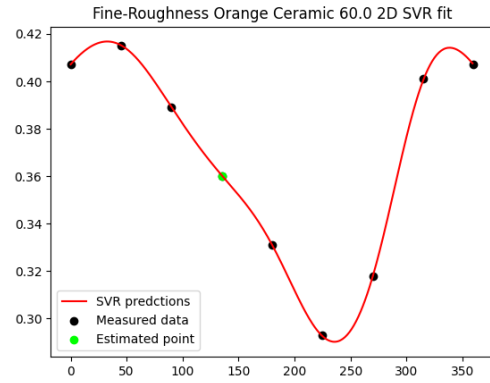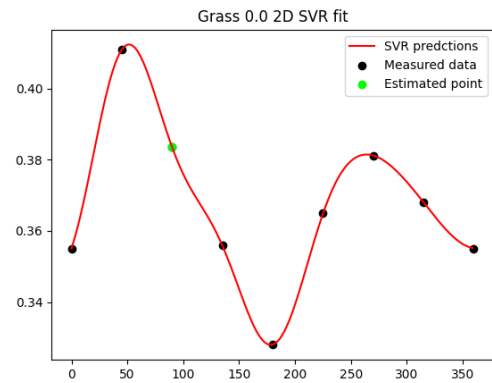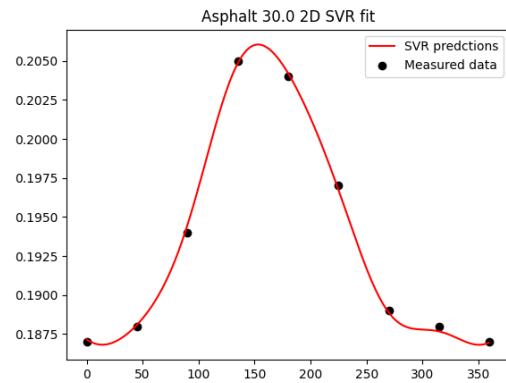

A)
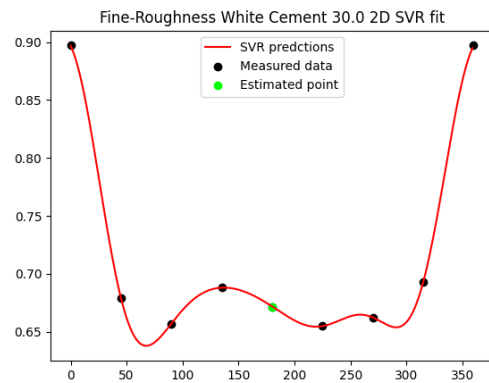
B)
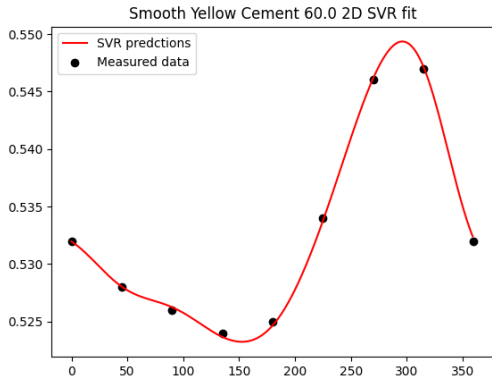
C)

D)

E)

F)

Figure 6) Example data fit to a 2D SVR algorithm

The x axis represents the azimuth angle in degrees, and the y axis represents the broadband reflectance. Due to the large difference in azimuth angle between each measurement, only one or two measurements per azimuth circle captured the highly reflective properties of the materials at the BRDF's maximum, and the 2D models weren't able to properly capture this behavior without overfitting to the measurements. properly capture this behavior without overfitting to the measurements.

After the 2D SVR model was applied, the sun's location was matched with the new dataset. For each calculated broadband reflectance value, he location of the sun which corresponded to the largest view angle that was smaller than the modelled one was added. This enhanced dataset was then passed to another SVR algorithm, which would take the angles of the sun and the measurement as inputs and use them to predict the broadband reflectance. Then, using the data that were withheld from the model fitting process, a Mean Absolut Error (MAE) and Mean Squared Error (MSE) value was calculated to validate the BRDF model. The final step was to use the values predicted by the model to calculate the albedo of the

material for the corresponding location of the sun. Since the albedo takes its largest value when the material reflects the highest amount of light, the BRDF for the zenith angle of the sun for which the model predicts the highest broadband reflectance values will be plotted. Then, the albedo will be calculated for various positions of the sun using the predictions of the models.

Results: These are the spectra that were gathered for each material:
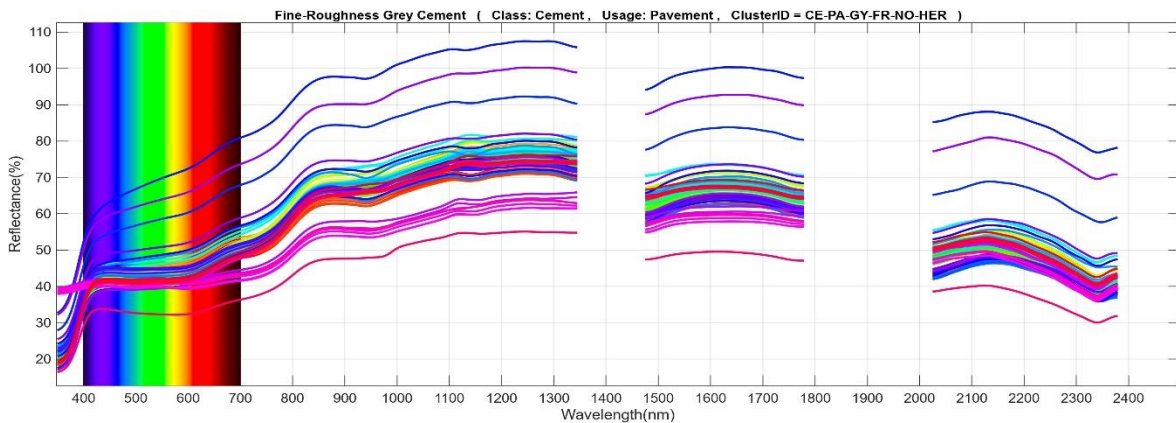

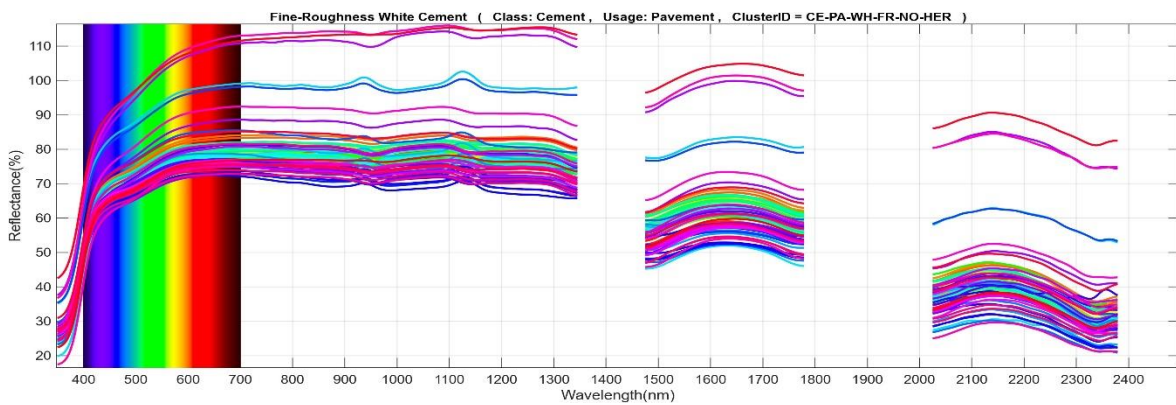*Figure 7) Gathered spectra for the fine-roughness grey cement plate*

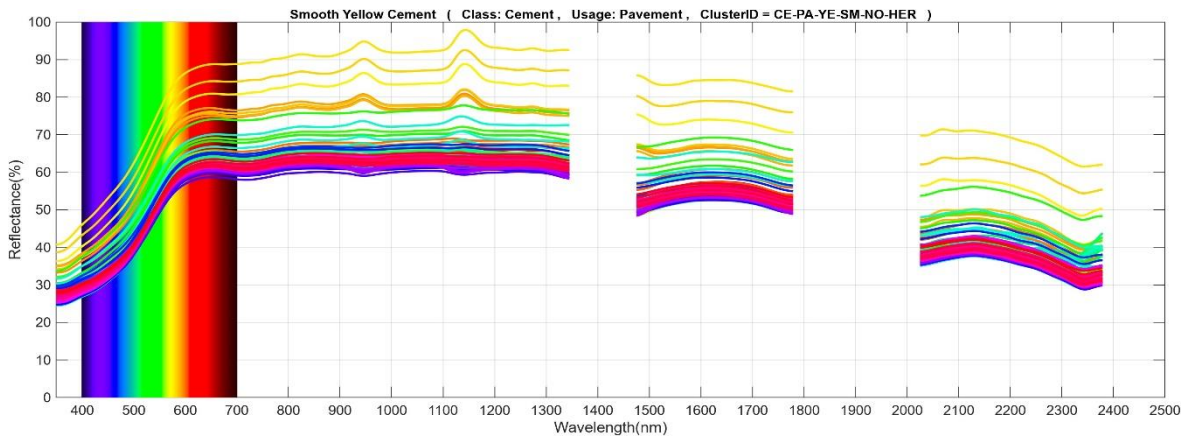*Figure 8) Gathered spectra for the fine-roughness white cement plate*

Figure 9) Gathered spectra for the smooth yellow cement plate
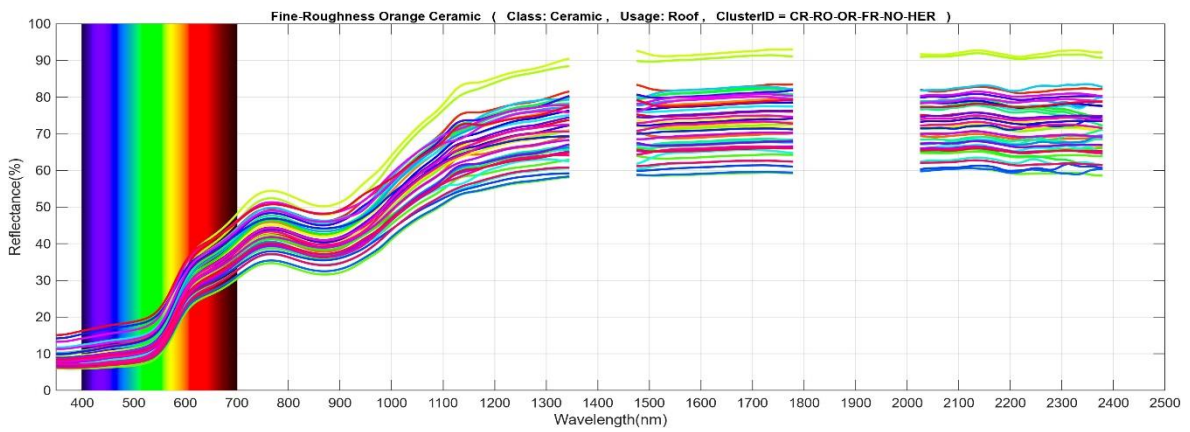

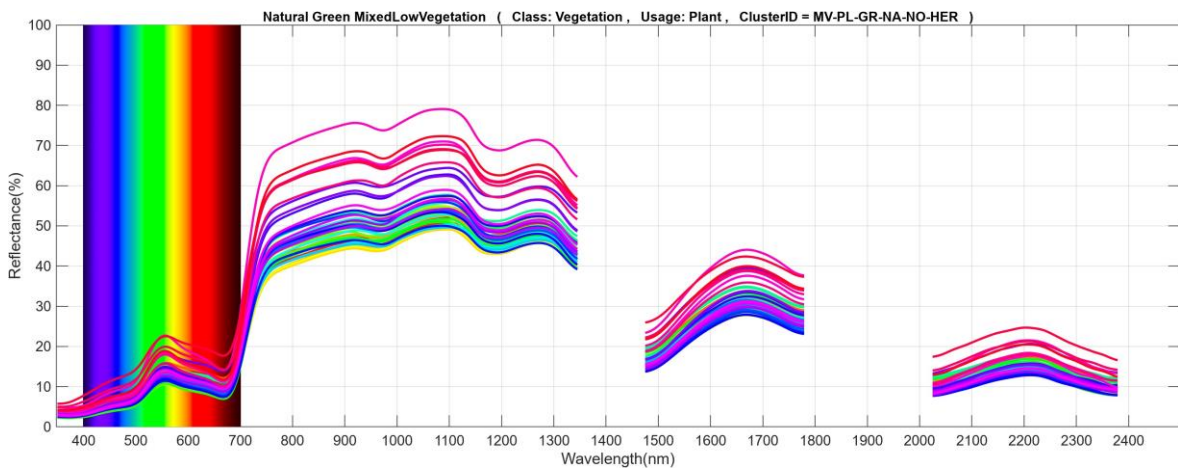*Figure 10) Gathered spectra for the fine-roughness orange ceramic surface*

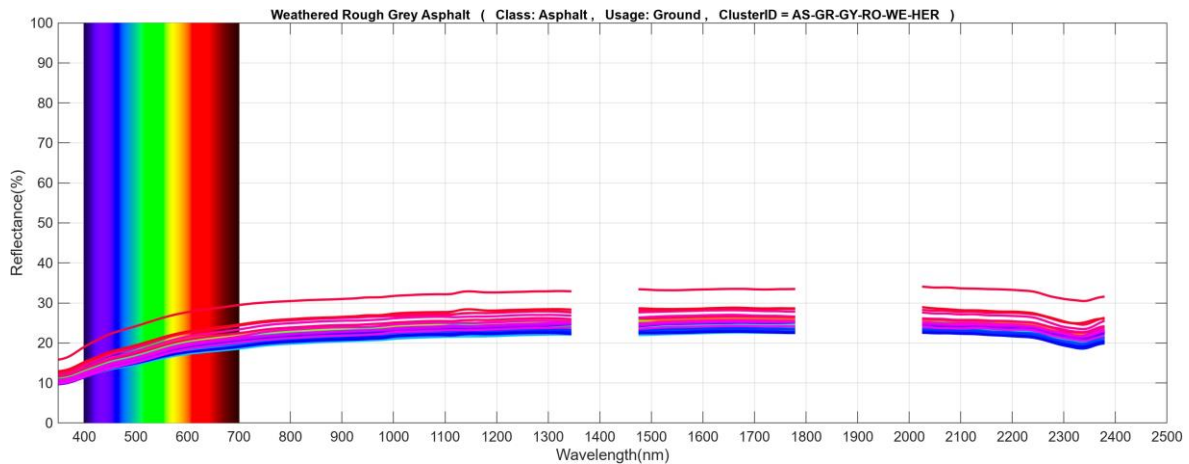*Figure 11) Gathered spectra for the grass*

Figure 12) Gathered spectra for the asphalt

The x axis shows the wavelength in nanometers, and the y axis shows the reflectance. The gaps in the spectra are the wavelengths that were removed due to the interference of the atmosphere. Each material's spectra show similar patterns of increasing and decreasing, but this pattern becomes more or less pronounced depending on the angles of the measurement.

It is apparent that every material is much more reflective in the infrared wavelengths than the visible spectrum, with the exception of the asphalt, which has mostly uniform reflectance. Also, for each material, despite the difference in the absolute values of spectral reflectance for each different measurement, they all follow a similar pattern, which is different for each material. Most of the measurements are grouped together at lower reflectances, with a few of them having much higher reflectances than the rest.

A key detail of some of the spectra is that for certain materials, certain wavelengths, and certain angles, the reflectance exceeds 100%. This is because the materials measured aren't diffuse, but reflect light speeularly,so more light may be reflected in one particular direction than by a Lambertian standard surface[9].

The most notable observation is the difference between the fine-roughness grey cement plate and the fine-roughness white cement plate. These two were made from the same material, with their only difference being their coat of paint. This difference has an impact on their respective spectra, the white material's reflectance at certain wavelengths and angles exceeds 110%, while the grey material's is always below this value. The difference in reflectance is very evident between 350 nm and 1345 nm, while in the rest of the spectrum there doesn't seem to be any significant difference in reflectance.

14

For the three cement plates, there is a pattern of increase in spectral reflectance while the wavelength increases from the visible to the infrared area, which then stabilizes at the infrared area, and slowly starts to decrease after the first gap. This is very different to the ceramic surface's behavior, which shows a slow but steady increase up until the first gap, and then stabilizes at high values. Furthermore, despite the difference in the observed surface of the ceramic plate, the pattern of the spectral reflectance remains similar for all measurements. Therefore, the surface of a material doesn't necessarily affect its spectral reflectance.

The grass's reflectance is relatively low in the visible spectrum, but significantly increases in the infrared range, and then significantly decreases again after the first removed spectral band. Its spectra are also more uniformly spread, they aren't gathered as densely at lower values as the rest of the materials, perhaps due to the complex surface. The asphalt has the lowest reflectances of all the materials, which is also very even across the whole spectrum.

The following plots are the resulting BRDF models for one location of the sun, along with their evaluation graphs. The rings represent the corresponding θ of the view position each point, and the radial axes represent the corresponding φ of the view position. The color of each point represents the broadband reflectance value predicted by the model for that point. These predictions can be used to calculate the albedo, using equations (8), (9), and (10).

A)

B)
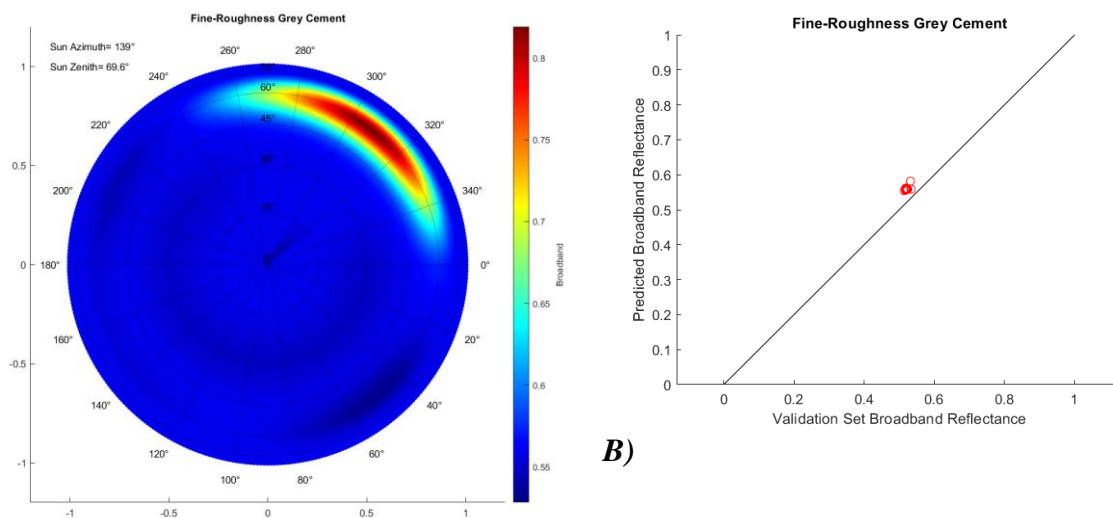
Figure 13) The BRDF model of the grey cement plate. A) shows the visual representation, and B) shows the evaluation plot of the model
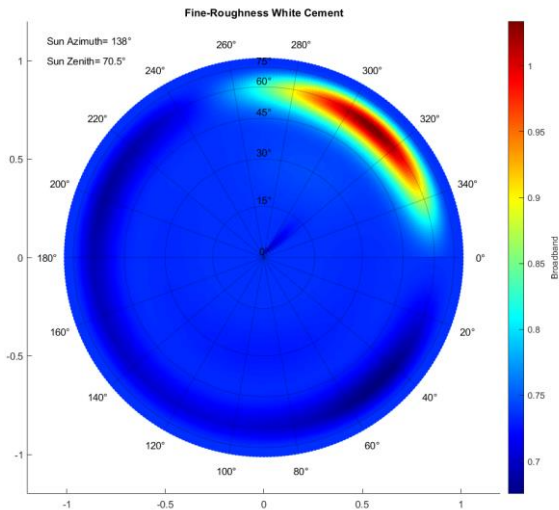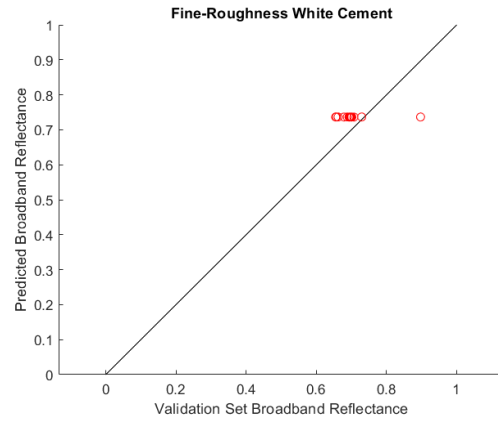
Figure 14) The BRDF model of the white cement plate. A) shows the visual representation, and B) shows the evaluation plot of the model

Figure 15) The BRDF model of the yellow cement plate. A) shows the visual representation, and B) shows the evaluation plot of the model
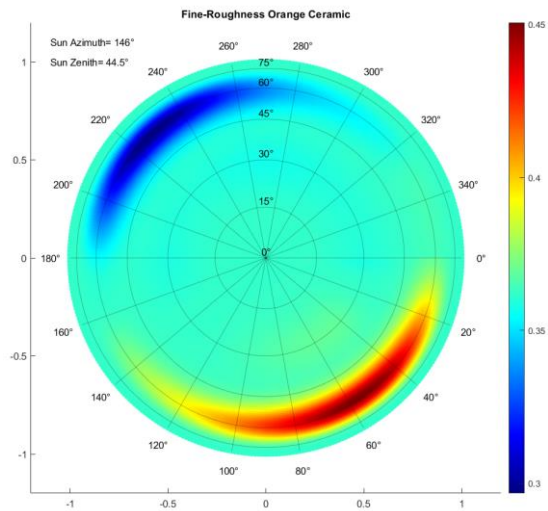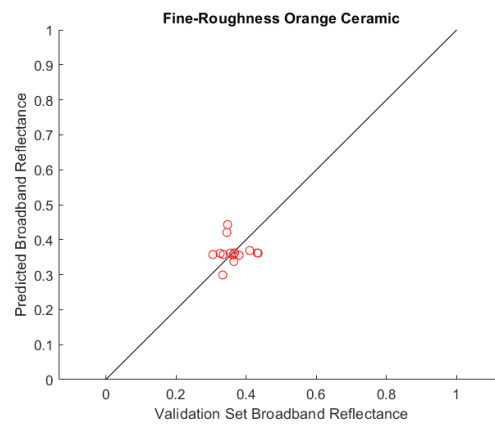
A)

Figure 16) The BRDF model of the ceramic surface. A) shows the visual representation, and B) shows the evaluation plot of the model
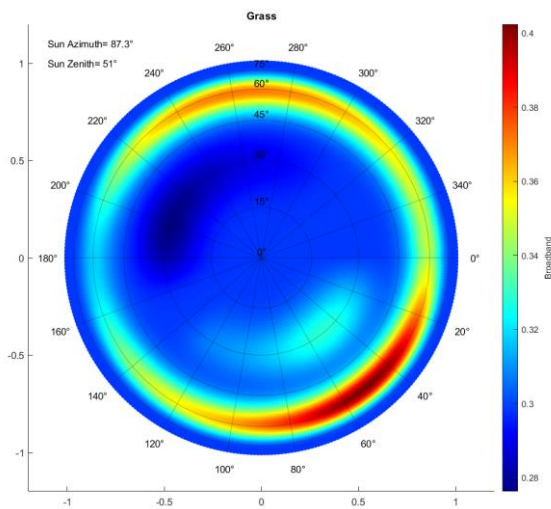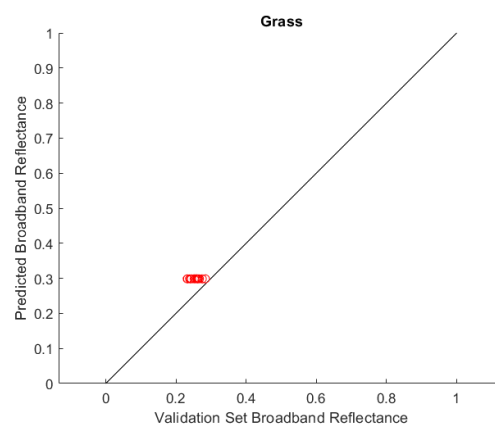
Figure 17) The BRDF model of the grass. A) shows the visual representation, and B) shows the evaluation plot of the model
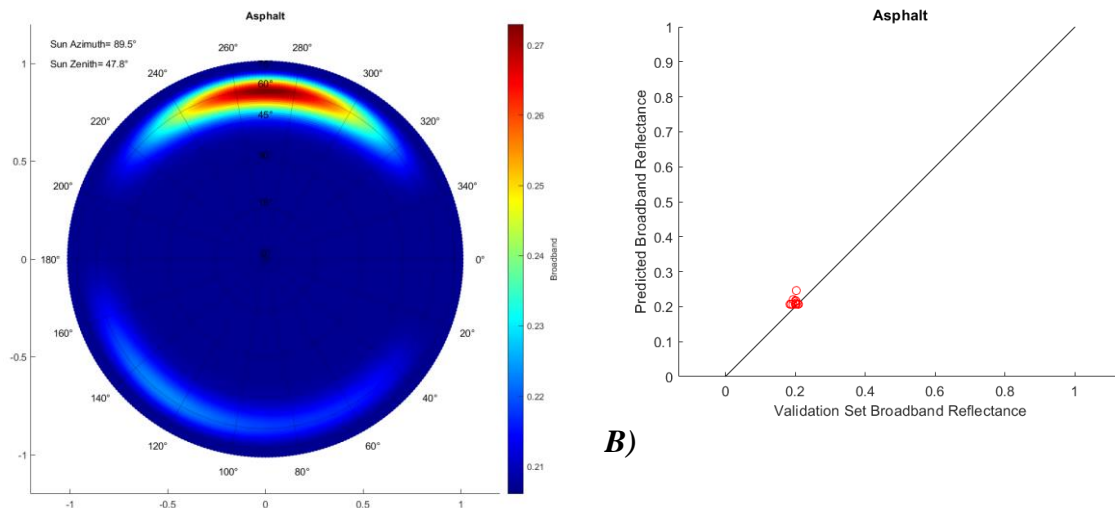
Figure 18) The BRDF model of the asphalt. A) shows the visual representation, and B) shows the evaluation plot of the model

The grey and white cement plates display very similar behaviors, which is unsurprising considering the two are made of the same material. They both have relatively constant values while the view is away from the same zenith angle as the sun and/or away from an azimuth angle opposite to that of the sun. What is surprising however is the difference in predicted values. This difference can be attributed entirely to their different coat of paint.
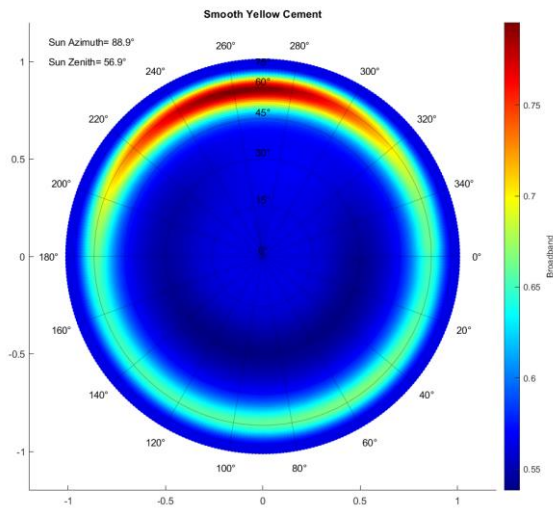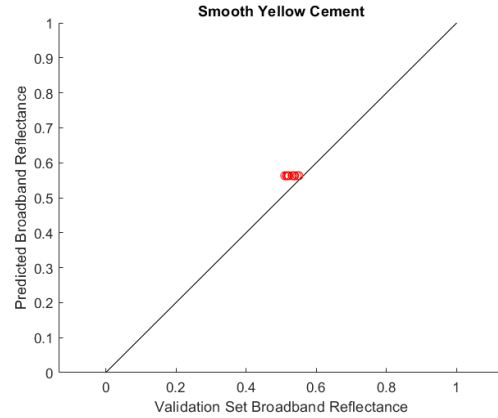
The BRDF model of the yellow plate shows an interesting behavior, where the maximum close to the sun's zenith angle and opposite to the sun's azimuth is consistent with the other two materials, however this material has a slightly elevated broadband reflectance when viewed from the same azimuth angle as the sun along the entire azimuth circle. This behavior is consistent with the original measurements.

The most interesting behavior is that of the BRDF of the ceramic plate. Instead of having a relatively stable value outside of opposite from the sun, here the material reaches its maximum broadband reflectance value in an azimuth angle that is close to the curved side closest to the sun, and in the opposite direction, the BRDF dips and reaches a minimum value. This happens because of the curved surface of the material. When the sun faces the curve of the material, there's a larger area able to reflect sunlight in that direction, and on the opposite side, the shape of the material blocks sunlight, so the broadband reflectance becomes a lot lower. This behavior was captured by the BRDF model, which shows that the BRDF isn't simply a function of the view angles and light source angles, but also the shape of the material.

The grass' BRDF displays a complex and irregular behavior, most likely due to its surface. Every grass blade is curved differently, some of them have been stepped on, and there are also small insects moving through it, which makes the way if reflects light very difficult to predict.

The asphalt's behavior is almost identical to the grey and white cement plates, with the only difference being that it's much darker.

Using the predictions of the models, the albedo values for various locations of the sun will be calculated using formulas (8), (9), and (10). The results are presented in the following board:

Grey Cement Plate	$\varphi_0 = 139, \theta_0 = 69.6: \alpha = 0.568$ $\varphi_0 = 133, \theta_0 = 60: \alpha = 0.555$ $\varphi_0 = 224, \theta_0 = 58: \alpha = 0.559$
White Cement Plate	$\varphi_0 = 138, \theta_0 = 70.5: \alpha = 0.742$ $\varphi_0 = 153, \theta_0 = 51: \alpha = 0.734$ $\varphi_0 = 225, \theta_0 = 60: \alpha = 0.735$
Yellow Cement Plate	$\varphi_0 = 88.9, \theta_0 = 56.9: \alpha = 0.593$ $\varphi_0 = 105, \theta_0 = 37: \alpha = 0.553$ $\varphi_0 = 131, \theta_0 = 22: \alpha = 0.557$
Ceramic Surface	$\varphi_0 = 146, \theta_0 = 44.5: \alpha = 0.364$ $\varphi_0 = 159, \theta_0 = 41: \alpha = 0.361$ $\varphi_0 = 177, \theta_0 = 39: \alpha = 0.361$
Grass	$\varphi_0 = 87.3, \theta_0 = 51: \alpha = 0.314$ $\varphi_0 = 122, \theta_0 = 22: \alpha = 0.290$ $\varphi_0 = 150, \theta_0 = 19: \alpha = 0.294$
Asphalt	$\varphi_0 = 89.5, \theta_0 = 49.8: \alpha = 0.211$ $\varphi_0 = 125, \theta_0 = 21: \alpha = 0.206$ $\varphi_0 = 160, \theta_0 = 14: \alpha = 0.204$

The albedo of all materials reaches a maximum value when the predicted broadband reflectance predictions also reach their maximum value, but the change in albedo for different sun locations is fairly small. It is worth noting that the largest albedo of the white cement plate is 34% higher than that of the grey cement plate, which is made from the same material, but has a different coating of paint.

The albedo of concretes ranges between 0.41 and 0.77[10]. The albedo of various types of grass ranges between 0.16 and 0.32[11]. The albedo of asphalt ranges between 0.12 and 0.23[12]. All of the albedos calculated in this work for these materials fall within their respective ranges. Two possible values for the albedo

of the ceramic surface are 0.42 and 0.24[13]. The highest albedo value calculated in this work is 0.364, which is 13% lower than 0.42, and 52% higher than 0.24.

Lastly, there are the evaluation plots and errors of the models. The x axis represents the broadband reflectance value of the evaluation dataset, and the y axis represents the broadband reflectance value predicted for the same point by the BRDF models. As explained earlier, these points were chosen at random, taking one random measured azimuth circle at $\theta=30°$, and one azimuth circle at $\theta=60°$, with the only criterion being that these azimuth circles do not contain the largest broadband reflectance value we measured. As a result, the measured broadband reflectance values are clustered together fairly closely for all materials, which is evidence that for these materials, the broadband reflectance value is relatively constant along random view angles. The errors of the models are the following:

Grey Cement Plate	Train MAE=0.008 Test MAE=0.04
	Train MSE=8e-5 Test MSE=0.002
White Cement Plate	Train MAE=0.009 Test MAE=0.06
	Train MSE=8e-5 Test MSE=0.004
Yellow Cement Plate	Train MAE=0.009 Test MAE=0.03
	Train MSE=9e-5 Test MSE=0.001
Ceramic Surface	Train MAE=0.009 Test MAE=0.04
	Train MSE=9e-5 Test MSE=0.002
Grass	Train MAE=0.01 Test MAE=0.04
	Train MSE=1e-4 Test MSE=0.002
Asphalt	Train MAE=0.008 Test MAE=0.01
	Train MSE=8e-5 Test MSE=0.0003

Taking the square root of the MSE value gives the Root Mean Squared Error (RMSE) value, which is the same as the MAE value. The models are fairly

accurate at predicting the values of the training dataset, and a bit less accurate at predicting other values.

Discussion: The albedo of a material is dependent on the properties of the material, the location of the sun, and the conditions of the atmosphere. The measurements were all conducted during whether that was either completely sunny, or with very few clouds and haze. However, the process of taking measurements for one material in one day can be very time consuming, so gathering enough measurements in one day may not always be realistic. The humidity and concentration of aerosols in the atmosphere also plays a part, because they interact with certain wavelengths and can be hard to compensate for.

In the measurement process there were large changes in both the azimuth and zenith angles of the radiometer, due to the inaccuracy in setting the angles. This made the use of 2D SVR algorithms invaluable in the calculation of the BRDF models, the initial dataset was too sparse to be properly fit to a SVR algorithm. An algorithm wasn't used to increase the zenith angle values because for these, at most three points per azimuth angle were available.

A way to improve the models could be to decrease the step in the azimuth and zenith angles of the radiometer, thus increasing the number of available measurements, but also make the measurement process much slower. In the winter, there are more clouds and haze, which are next to non-existent in the summer. However, in the summer there's more precipitable water. Taking measurements in the summer is preferable, because the variations in incident radiance caused by precipitable water are much smaller than those caused by moving clouds and haze. During the summer, the sun's zenith angle changes much faster than the winter, and this makes it very important to keep the measurement process as fast as possible. In both the summer and the winter however, during the noon the sun's zenith angle remains relatively stable, so this is an ideal time to take measurements, and model the BRDF only for that position of the sun.

The SVR algorithms weren't the only methods considered for modeling the BRDF of the materials. Another idea was to approximate the measurements with a higher dimension ellipsoid surface. This didn't work due to issues with fitting algorithms. Looking at the final model of the ceramic plate, it's also evident that it cannot be approximated by an ellipsoid, as these surfaces do not have any minima.

Conclusion: Using a hyperspectral radiometer in order to measure the spectral reflectance of various materials under direct sunlight, BRDF models were created and used to calculate their albedo. These models can predict the broadband reflectance values close to view zenith angles that were measured fairly well, however their ability to do so under different view zenith angles remains to be tested. Comparing the spectral reflectance and broadband reflectance measurements, an impact of the paint of a material on its reflective properties can be seen, which can potentially increase its albedo value as much as 34% for certain materials. The BRDF models have displayed a clear correlation between broadband reflectance and the shape of a material's surface. These findings underscore the importance of considering surface treatments in urban planning and design, as they can substantially influence the thermal and optical properties of building materials, potentially affecting urban microclimates and energy consumption. Based on the impact of paint on the albedo, painting buildings white can increase their albedo, thus improving their heat insulation. The shape of the rooves of buildings can also be designed its effect on the BRDF in mind, increasing their broadband reflectance and their albedo based on the orientation of the building. The next steps of this work will be to model the BRDF separately for each wavelength of the spectral reflectance. These models can be used to adjust the hyperspectral measurements to match the respective multispectral satellite sensors (e.g., Sentinel-2 [14]), considering the specific satellite and sun angles, which can play a significant role in satellite image classification.

References:

1. Rocha, Alby Duarte, et al. "Unprivileged groups are less served by green cooling services in major European urban areas." *Nature Cities* (2024): 1-12.
2. Coakley, J. A. "Reflectance and albedo, surface." *Encyclopedia of atmospheric sciences* 12 (2003).
3. Bergstrom, Robert W., et al. "Spectral absorption properties of atmospheric aerosols." *Atmospheric Chemistry and Physics* 7.23 (2007): 5937-5943.
4. Lantzanakis, Giannis, et al. "Initial development of the urbisphere urban hyperspectral library: Berlin, Germany." *2023 Joint Urban Remote Sensing Event (JURSE)*. IEEE, 2023.
5. Ward, Gregory J. "Measuring and modeling anisotropic reflection." *Proceedings of the 19th annual conference on Computer graphics and interactive techniques*. 1992.
6. Müller, Ch, Brian Hosgood, and Giovanni Andreoli. "Sensitivity analysis and quality assessment of laboratory BRDF data." *Remote Sensing of Environment* 64.2 (1998): 176-191.
7. Ranson, K. J., J. R. Irons, and C. S. T. Daughtry. "Surface albedo from bidirectional reflectance." *Remote sensing of Environment* 35.2-3 (1991): 201-211.
8. Smola, Alex J., and Bernhard Schölkopf. "A tutorial on support vector regression." *Statistics and computing* 14 (2004): 199-222.
9. Winther, Jan-Gunnar. "Spectral bi-directional reflectance of snow and glacier ice measured in Dronning Maud Land, Antarctica." *Annals of Glaciology* 20 (1994): 1-5.
10. Levinson, Ronnen, and Hashem Akbari. "Effects of composition and exposure on the solar reflectance of portland cement concrete." *Cement and concrete research* 32.11 (2002): 1679-1698.

11. Zvomuya, Francis, et al. "Surface albedo and soil heat flux changes following drilling mud application to a semiarid, mixed-grass prairie." *Soil Science Society of America Journal* 72.5 (2008): 1217-1225.
12. Sen, Sushobhan, and Jeffery Roesler. "Aging albedo model for asphalt pavement surfaces." *Journal of Cleaner Production* 117 (2016): 169-175.
13. Levinson, Ronnen, et al. "Experimental comparison of pyranometer, reflectometer, and spectrophotometer methods for the measurement of roofing product albedo." *Solar Energy* 206 (2020): 826-847.
14. Muller-Wilm, Uwe, et al. "Sentinel-2 level 2A prototype processor: Architecture, algorithms and first results." *Proceedings of the ESA Living Planet Symposium, Edinburgh, UK.* 2013.

Appendix - Code:

Below is the code that was written as part of this work. It is separated in four segments. The first segment reads the measured radiance of the radiometer and plots it. The second segment is responsible for the pre-processing, it splits the train and validation datasets, and applies the 2D SVR algorithm to the train dataset. The third segment fits the BRDF model, performs all error calculations, and plots the model's predictions for the sun's location which produces the highest broadband reflectance predictions. The last segment which calculates the albedo of the material.

The first code segment is written in python.

```python
'''LIBRARIES'''

import matplotlib.pyplot as plt

import numpy as np

import os

# pip install pandas

import pandas as pd


os.chdir(r'the directory containing the measurements')

f=open('a file containing measurements')

measurements=open('a text file that helps with the formatting of the
measurements','r+')


# Remove unnecessary lines


i=1

for x in f.readlines():

    if(i>26):
```

23

```python
        measurements.write(x)

    i+=1


f.close()

measurements.close()

df=pd.read_csv('the text file',sep='\t')


x=df['Wvl'].values

y=df['Rad. (Target)'].values

fig=plt.figure(figsize=(10,5))

plt.plot(x,y,color='green')

plt.xlabel('Wavelength (nm)')

plt.ylabel('Radiance (W/m^2/sr/nm)')

plt.ylim(0,0.32)

plt.show()
```

The second code segment is written in python

```python
'''LIBRARIES'''

import matplotlib.pyplot as plt

import numpy as np

# pip install pandas

import pandas as pd

# pip install scikit-learn

from sklearn.svm import SVR

'''FUNCTIONS'''

def read_angles(xlsx_folder,xlsx_filename):

    # Read the file

    path=xlsx_folder+"\\"+xlsx_filename

    df=pd.read_excel(path)


    # Access relevant values

    broadband=df['Broadband'].values

    X=df[['SunAz','SunEl','MesAz','MesEl']].values
```

24

```python
    return X,broadband
def zenith_splitter(X,broadband):
x=np.zeros(4)
x_90=np.zeros(4)
y=[0]
y_90=[0]

for i in range(0,len(X[:,3])):
if(X[i,3]!=90):
x=np.vstack((x,X[i]))
y=np.append(y,broadband[i])
else:
x_90=np.vstack((x_90,X[i]))
y_90=np.append(y_90,broadband[i])

x=np.delete(x,(0,1,2,3)).reshape(-1,4)
y=np.delete(y,0)
x_90=np.delete(x_90,(0,1,2,3)).reshape(-1,4)
y_90=np.delete(y_90,0)

return x,y,x_90,y_90
def circle_splitter(X,broadband,for_validation):
for i in range(0,len(for_validation)):
for_validation[i]-=1
print(for_validation)

reset_indices = np.where(X[:, 2] == 0)[0]

filtered_data = []
filtered_array_1d = []
validation_x=[]
```

```python
validation_y=[]


for i in range(len(reset_indices)):
start_idx=reset_indices[i]
if i == len(reset_indices) - 1:
end_idx = len(X)
else:
end_idx = reset_indices[i + 1]


if i not in for_validation:
start_idx = reset_indices[i]
print('Didn\'t remove circle',i+1)


filtered_data.extend(X[start_idx:end_idx, :])
filtered_array_1d.extend(broadband[start_idx:end_idx])
else:
print('Removed circle',i+1)
validation_x.extend(X[start_idx:end_idx, :])
validation_y.extend(broadband[start_idx:end_idx])


filtered_data_array = np.array(filtered_data)
filtered_array_1d = np.array(filtered_array_1d)
validation_x=np.array(validation_x)
validation_y=np.array(validation_y)


return filtered_data_array,filtered_array_1d,validation_x,validation_y
def buffed_2d_svr(x,y,material):
x=np.vstack((x,[0,0,0,0]))
y=np.append(y,0)


# print(x)
```

```python
name=material[:-5]


a=x[:,2].copy()

x_2d_final=np.zeros((1,4))

x_1d_final=[0]

y_final=[0]


x_placeholder=0

y_placeholder=y[0]

zzz=0

# Controls whether the additional estimated point will be displayed

estimated_point_display=0


# Variabl which helps with adding all the angles to the final matrix

f=0


for i in range(1,len(a)):

if(a[i]!=0):

x_placeholder=np.append(x_placeholder,a[i])

y_placeholder=np.append(y_placeholder,y[i])

else:

zzz+=1


for j in range(1,len(x_placeholder)):

if(abs(x_placeholder[j]-x_placeholder[j-1])!=45):

estimated_point_display=1

x_placeholder=np.append(x_placeholder,np.average((x_placeholder[j],x_placeholder[j
-1])))

y_placeholder=np.append(y_placeholder,np.average((y_placeholder[j],y_placeholder[j
-1])))

break
```

```python
x_placeholder=np.append(x_placeholder,360)

y_placeholder=np.append(y_placeholder,y_placeholder[0])


# SVR model

model=SVR(epsilon=0.00001,gamma=0.0005)

result=model.fit(x_placeholder.reshape(-1,1),y_placeholder)


# Predicted values

x_tba=np.arange(0,360,1)

y_tba=result.predict(x_tba.reshape(-1,1))


x_placeholder=np.delete(x_placeholder,-1)

y_placeholder=np.delete(y_placeholder,-1)


# print(x[i])


plt.plot(x_tba,y_tba,color='#ff0000',label='SVR predctions')

plt.scatter(x_placeholder,y_placeholder,color='#000000',label='Measured data')

plt.scatter(360,y_placeholder[0],color='#000000')


if (estimated_point_display==1):

plt.scatter(x_placeholder[-1],y_placeholder[-1],color='#00ff00',label='Estimated
point')


plt.title(name+' '+str(x[i,3])+' 2D SVR fit')

plt.legend()

plt.show()


if (zzz>=1):
# Taking the predicted values

x_1d_final=np.concatenate((x_1d_final,x_tba))

y_final=np.concatenate((y_final,y_tba))
```

```python
estimated_point_display=0

for k in x_tba:

if k<x[f+1,2] or x[f,2]==315:

pl=[x[f,0],x[f,1],k,x[f,3]]

x_2d_final=np.vstack((x_2d_final,pl))

else:

f+=1

pl=[x[f,0],x[f,1],k,x[f,3]]

x_2d_final=np.vstack((x_2d_final,pl))


f+=1


x_placeholder=0

y_placeholder=y[i]


x_2d_final=np.delete(x_2d_final,(0,1,2,3)).reshape(-1,4)

y_final=np.delete(y_final,0)


return x_2d_final,y_final

def buffed_plus_90(x_buffed,y_buffed,x_90,y_90):

x_tot=np.vstack((x_buffed,x_90))

y_tot=np.hstack((y_buffed,y_90))


for i in range(0,len(y_tot)):

x_tot[i,1]=90-x_tot[i,1]

x_tot[i,3]=90-x_tot[i,3]


return x_tot,y_tot

def save_buffed_predictions(X,Y,x_test,y_test,xlsx_filename,output_folder):


name=xlsx_filename[:-5]+' NEWfed SVR measurements.xlsx'
```

```python
data_train={
'SunAz':X[:,0],
'SunEl':X[:,1],
'MesAz':X[:,2],
'MesEl':X[:,3],
'Broadband':Y
}


data_test={
'SunAz':x_test[:,0],
'SunEl':x_test[:,1],
'MesAz':x_test[:,2],
'MesEl':x_test[:,3],
'Broadband':y_test
}


df_1=pd.DataFrame(data_train)
df_2=pd.DataFrame(data_test)


df_1.to_excel(excel_writer=output_folder+'\\'+xlsx_filename[:-5]+' train dataset.xlsx')
print('Training data saved as',xlsx_filename[:-5]+' train dataset.xlsx')
df_2.to_excel(excel_writer=output_folder+'\\'+xlsx_filename[:-5]+' test dataset.xlsx')
print('Test data saved as',xlsx_filename[:-5]+' test dataset.xlsx')


'''CODE EXECUTION'''
xlsx_folder=r"the directory of the file that contains the broadband reflectances"
xlsx_filename="the file that contains the broadband reflectances"
output_folder=r"the directory were the new data will be stored"


X, brdf = read_angles(xlsx_folder=xlsx_folder, xlsx_filename=xlsx_filename)
```

```
x,y,x_90,y_90=zenith_splitter(X,brdf)
```

```
x_train,y_train,x_test,y_test=circle_splitter(x,y,[a list with the circles that
will be used for validation])
```

```
x_buffed,y_buffed=buffed_2d_svr(x_train,y_train,xlsx_filename)
```

```
X_full,BRDF_full=buffed_plus_90(x_buffed,y_buffed,x_90,y_90)
```

```
save_buffed_predictions(X_full,BRDF_full,x_test,y_test,xlsx_filename,output_folder
)
```

The third code segment is written in matlab

```
%% Inputs
```

```
xlsx_folder = 'the directory with the datasets that will be used for the BRDF
models';
```

```
xlsx_train = 'the file containing the data that the BRDF model will be fit to';
```

```
xlsx_test='the file containing the data that will be used to validate the model';
```

```
az = 18; % the user requested azimuth angle
```

```
%%
```

```
LjAdd_Path();
```

```
%%
```

```
name = extractBefore(xlsx_train, strlength(xlsx_train) - 18);
```

```
A = LjRead( xlsx_folder , xlsx_train );
```

```
A(1,:) = [];
```

```
test_dataset=LjRead(xlsx_folder,xlsx_test);
```

```
test_dataset(1,:)=[];
```

```
[maxValue, rowIndex] = max(A(:, 6));
```

```matlab
best_az=A(rowIndex,2);
ze=A(rowIndex,3);


X = A(:,2:5);
Y = A(:,6);


x_test=test_dataset(:,2:5);
y_test=test_dataset(:,6);


svr_model = LjTrain_CSVR(X,Y,100,10,0.01);
Y2 = LjApply_SVR(svr_model,X);


y_pred=LjApply_SVR(svr_model,x_test);


resol = 360;
AZ = zeros(resol,1)+best_az;
ZE = zeros(resol,1)+ze;


X2 = zeros(1,4);
c = 0;
for m = 1:1:89
    for n = 0:1:359
        c = c + 1;
        X2(c,1) = best_az;
        X2(c,2) = ze;
        X2(c,3) = n;
        X2(c,4) = m;
    end
end


BRDF = LjApply_SVR(svr_model,X2);
```

```matlab
%% Ectract model results
model_result_values(:,1:4)=X2;
model_result_values(:,5)=BRDF;


model_filename=[name,' SVR results.xlsx'];
writematrix(model_result_values,model_filename);
%% Plots
figure;
hold on;
axis equal;
plot([0 1],[0 1],'k-');
plot(y_test,y_pred,'or');
xlabel('Validation Set Broadband Reflectance');
ylabel('Predicted Broadband Reflectance');
title(name);


MAE_train=mean(abs(Y-Y2));
MSE_train=mean((Y-Y2).^2);
disp(['MAE train=',num2str(MAE_train)]);
disp(['MSE train=',num2str(MSE_train)]);


MAE_test=mean(abs(y_test-y_pred));
MSE_test=mean((y_test-y_pred).^2);
disp(['MAE test=',num2str(MAE_test)]);
disp(['MSE test=',num2str(MSE_test)]);


R = BRDF;


X_KART = sind(X2(:,4)).*cosd(X2(:,3));
Y_KART = -sind(X2(:,4)).*sind(X2(:,3));
%% Rotation
% Rotation matrix for counterclockwise rotation
```

```matlab
Rotation_matrix = [cosd(-best_az+az), sind(-best_az+az);
    -sind(-best_az+az), cosd(-best_az+az)];


% Apply rotation to points
rotated_points_1 = (Rotation_matrix * [X_KART Y_KART]')';
%% 2d representation


sun_az=num2str(az);
sun_ze=num2str(ze);


figure;
scatter(rotated_points_1(:,1),rotated_points_1(:,2),[],BRDF,'filled');
hold on;
cb = colorbar;
ylabel(cb,'Broadband','FontSize',16);
colormap('jet');
axis equal;
xlim([-1.2 1.2]);
ylim([-1.2 1.2]);


title(name);
text(-1.1,1.1,['Sun Azimuth= ',sun_az '°']);
text(-1.1,1,['Sun Zenith= ',sun_ze '°']);


transparency=0.3;


theta = linspace(0, 2*pi, 360);
angles = 0:15:80;


for angle = angles
    r = sind(angle);
    xCircle = r * cos(theta);
```

```matlab
    yCircle = r * sin(theta);

    plot(xCircle, yCircle, 'k', 'Color', [0 0 0 transparency]);


    text(0, r, [num2str(angle) '°'], 'HorizontalAlignment', 'center',
'VerticalAlignment', 'bottom');
end


angles = 0:20:350;

for angle = angles

    xLine = [0 cosd(angle)];

    yLine = [0 sind(angle)];

    plot(xLine, yLine, 'k', 'Color', [0 0 0 transparency]);


    xText = 1.1 * cosd(angle);

    yText = 1.1 * sind(angle);

    if angle>0

        text(xText, yText, [num2str(360-angle) '°'], 'HorizontalAlignment',
'center', 'VerticalAlignment', 'middle');

    else

        text(xText, yText, [num2str(angle) '°'], 'HorizontalAlignment', 'center',
'VerticalAlignment', 'middle');

    end

end
```

The last code segment was written in python

```python
'''LIBRARIES'''

import numpy as np

# pip install pandas

import pandas as pd


'''FUNCTIONS'''


def read_svr_results(xlsx_folder,xlsx_filename):

    # Read the file
```

```python
    path=xlsx_folder+"\\"+xlsx_filename

    df=pd.read_excel(path,header=None)

    df.columns=['SunAz','SunEl','MesAz','MesEl','BRDF']


    values=df[['SunAz','SunEl','MesAz','MesEl','BRDF']].values


    return values


def first_sum(data):
    reset_indices = np.where(data[:, 2] == 0)[0]


    results = []


    for i in range(len(reset_indices)):
        start_idx = reset_indices[i]


        if i == len(reset_indices) - 1:
            end_idx = len(data)
        else:
            end_idx = reset_indices[i + 1]


        period_sum = np.sum(data[start_idx:end_idx, 4])/360


        constant_value = data[start_idx, 3]


        results.append([period_sum, constant_value])


    results=np.array(results)
    return results


def second_sum(values,angles):
    result=0
```

```python
    for i in range(1,len(angles)):

        dwi=np.sin(np.deg2rad(angles[i]))**2-np.sin(np.deg2rad(angles[i-1]))**2

        dwi*=np.pi


        result+=values[i-1,0]*dwi


    result/=np.pi
    return result


'''CODE EXECUTION'''


xlsx_folder=r'the directory of the file that contains the values predicted by the
BRDF model'

xlsx_filename=r' the file that contains the values predicted by the BRDF model '


values=read_svr_results(xlsx_folder,xlsx_filename)


theta=np.arange(0,90,1.0)


for i in range(0,len(theta)):
    theta[i]+=0.5


sums1=first_sum(values)
# print(sums1)

# print(theta)


albedo=second_sum(sums1,theta)


print(xlsx_filename[:-17],'albedo =',albedo)
```